Insolation and CO_2 impacts on the spatial differences of the MIS-9 and MIS-11 climate between monsoonal China and central Asia

Hao Lu[1,2], Qiuzhen Yin[3], Zhipeng Wu[1,3], Feng Shi[1], Qingzhen Hao[1], Dunsheng Xia[4] and Zhengtang Guo[1]

1. key Laboratory of Cenozoic Geology and Environment, Institute of Geology and Geophysics, Chinese Academy of Sciences, Beijing, China; 2. Facluty of Geosciences, Utrecht University, Utrecht, the Netherlands; 3. Georges Lemaître Centre for Earth and Climate Research, Earth and Life Institute, Université Catholique de Louvain, Louvain-La-Neuve, Belgium; 4. Key Laboratory of West China's Environmental System (Ministry of Education), College of Earth and Environmental Sciences, Lanzhou University, Lanzhou, China

Corresponding author: H. Lu, luh@mail.iggcas.ac.cn

1. Introduction

There exists in strong regional diversity regarding the MIS-9 climate between monsoonal China and southern central Asia.

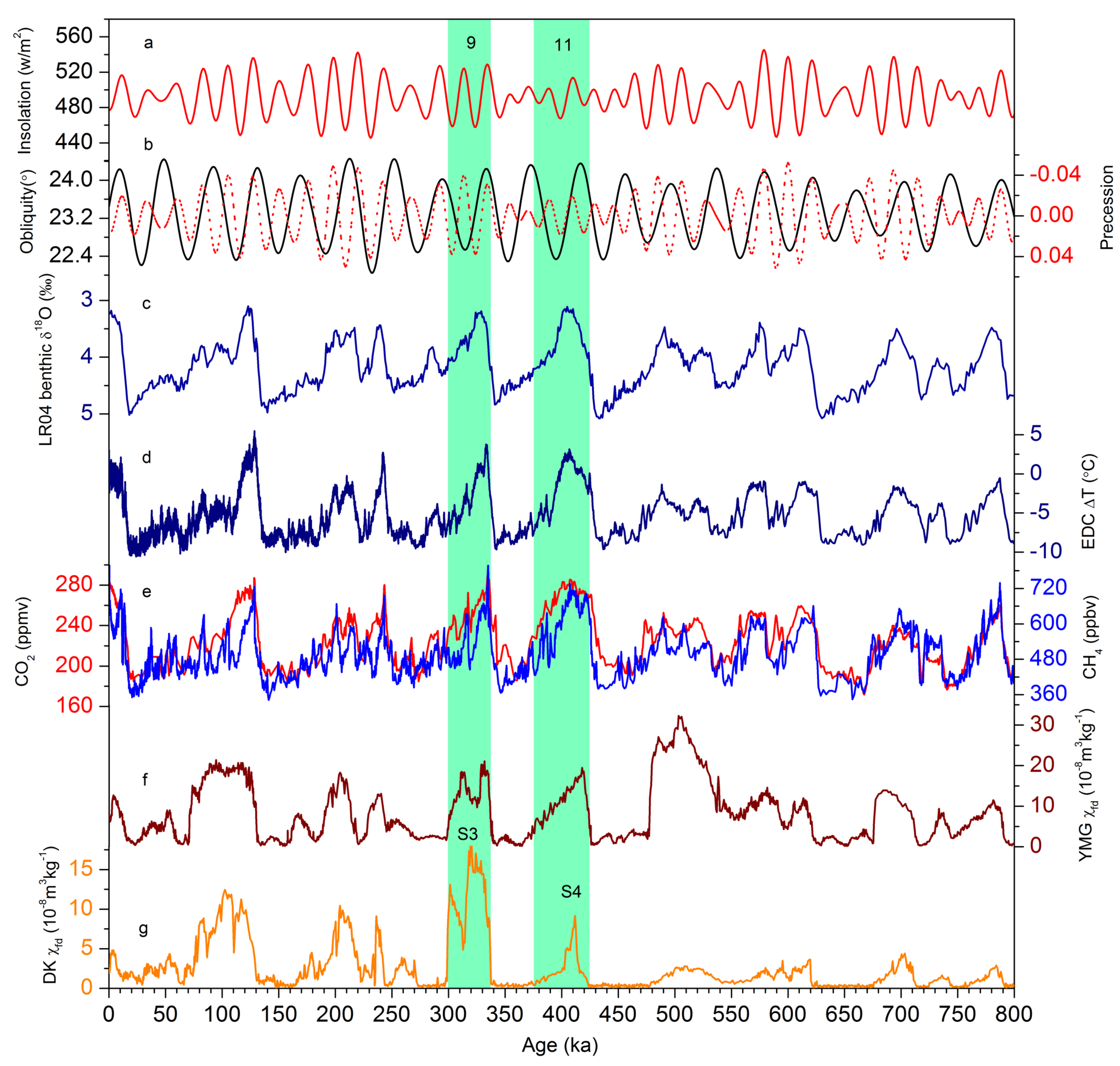

Figure 1. Comparison of frequency-dependent magnetic susceptibility (χ_{fd}) for Tajikistan loess in central Asia (the Darrai Kalon (DK) section) and the Chinese loess (the Yimaguan (YMG) section) with ice, marine and Earth's orbital records of the last 800 ka. (a) 21 June insolation 65˚N (Berger, 1978); (b) Earth's obliquity and precession parameters (Berger, 1978) on a reversed scale; (c) Marine $\delta^{18}O$ record (Lisiecki & Raymo, 2005) with the interglacial oxygen isotope stages (MIS) 11 and 9 labeled at top part; (d) Antarctic temperature (EDC) record (Jouzel et al., 2007); (e) CO_2 records (red) (Lüthi et al., 2008) and Antarctic CH_4 (blue) (Loulergue et al., 2008); (f) loess χ_{fd} at YMG, located in the central Chinese Loess Plateau (CLP) (Hao et al., 2012), and (g) DK, located in the Tajikistan ((Jia et al., 2018) with the S4 and S3 paleosol units labeled. The interglacials MIS-9 and MIS-11 are highlighted by light green shaded bars.

2. Model and experiments design

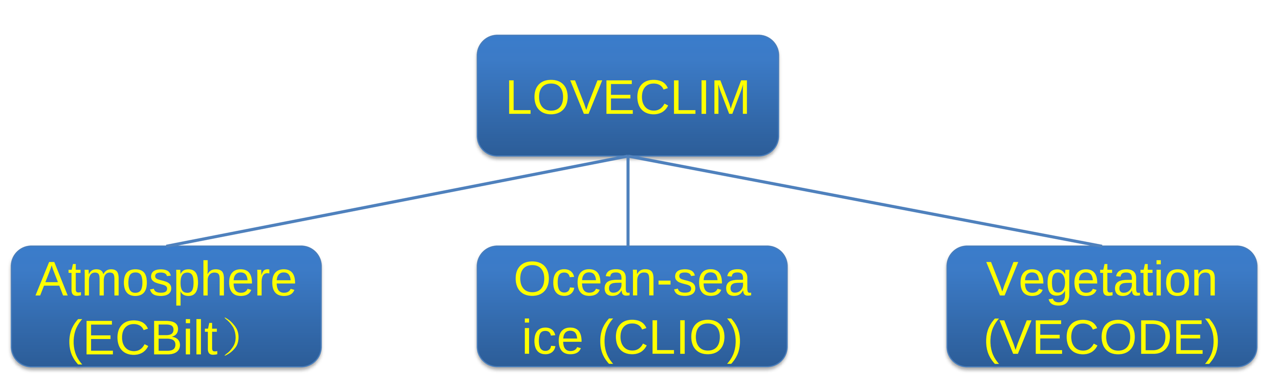

Table 1. Astronomical parameters (Berger 1978) and GHG concentrations of the control experiments for MIS-11 and MIS-9 (Yin and Berger, 2010).

MIS	Dates of $\delta^{18}O$ peaks (Ka BP)	Astronomical parameters			Dates of CO_2 peaks	CO_2eq (ppmv)
		Dates (ka BP)	Eccentricity	Obliquity		
MIS-9	329	334	0.031539	24.239	333	300
MIS-11	405	409	0.019322	23.781	407.5	286

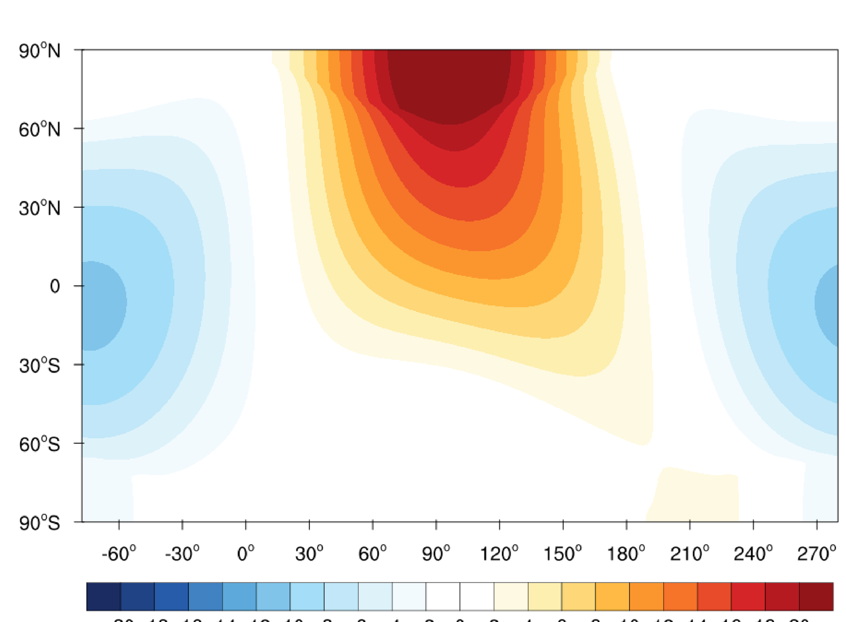

Figure 2. Difference in the distribution of insolation (W m-2) between the interglacials MIS-9 (334 ka) and MIS-11 (409 ka). The label on the x axis indicates true longitude of the Sun from the beginning to the end of the year (0˚ and 180˚ are for the spring and autumn equinoxes; 90˚ and 270˚ are for summer and winter solstices). Insolation is calculated from the long-term variations of eccentricity, precession and obliquity (Berger, 1978).

The factor separation method (Stein and Alpert, 1993) was used to separate the individual roles of insolation and GHG.

Individual impact of insolation $\widehat{f_{10}} = f_{10} - f_{00}$ $\qquad$ f_{00}: reference experiment

Individual impact of GHG $\widehat{f_{01}} = f_{01} - f_{00}$

Their combined effects $\widehat{f_{11}} = f_{11} - (f_{10} + f_{01}) = f_{11} - f_{00} - \widehat{f_{10}} - \widehat{f_{01}}$

The model experiments have been finished by Yin and Berger, 2012.

3. Results and Discussion

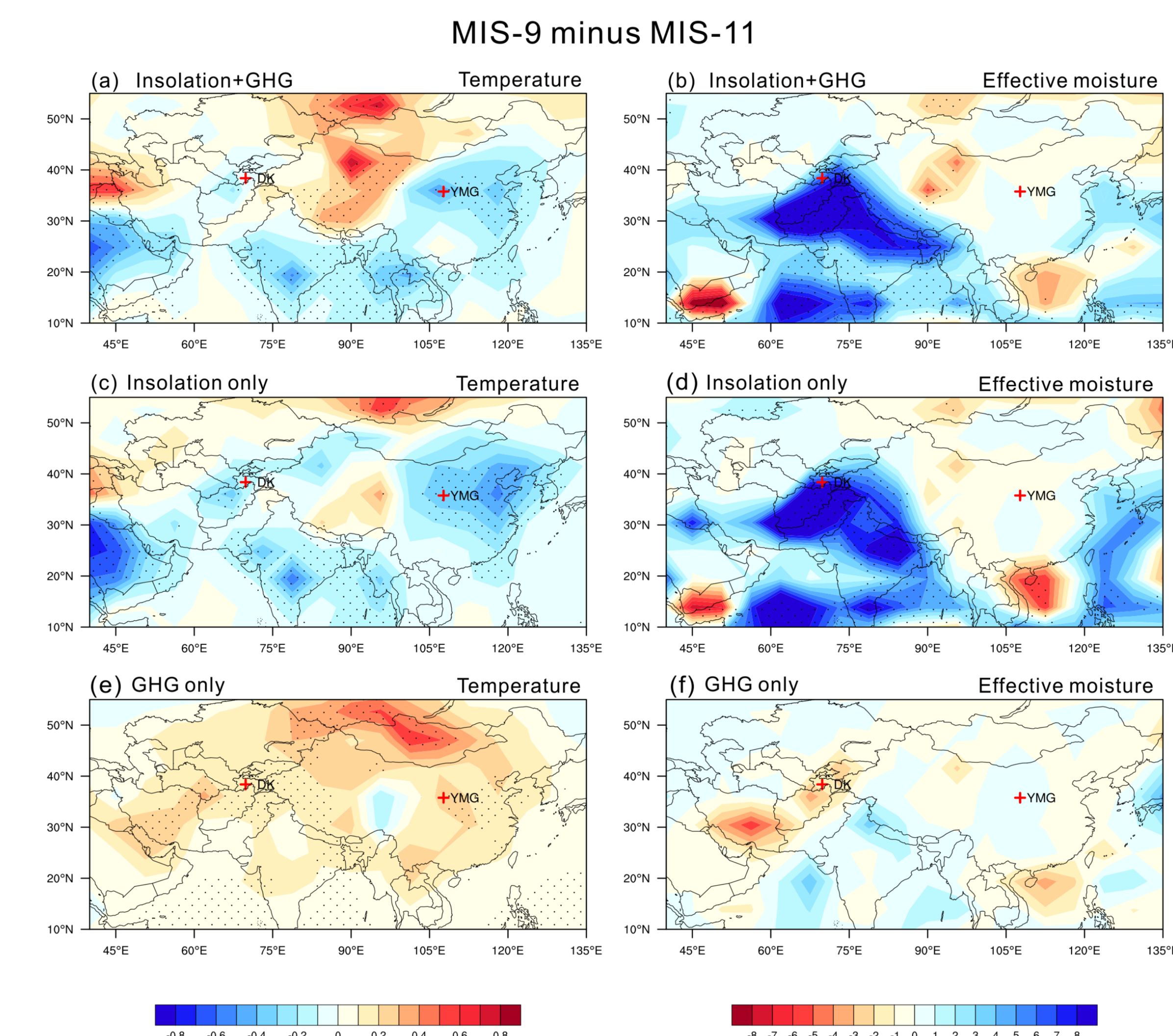

Figure 3. Spatial differences of the annual mean temperature (˚C) and effective moisture (precipitation minus evaporation) (cm/yr) between interglacials MIS-9 and MIS-11, respectively, (a) and (b) under the combined effects of insolation and GHG, (c) and (d) of insolation only, and (e) and (f) of GHG only. The red color represents higher temperature in (a), (c) and (e), and the blue color represents higher precipitation in (b), (d) and (f). Dotted regions indicate that changes are significant at the 0.05 confidence level. The red cross represents DK and YMG sections, respectively.

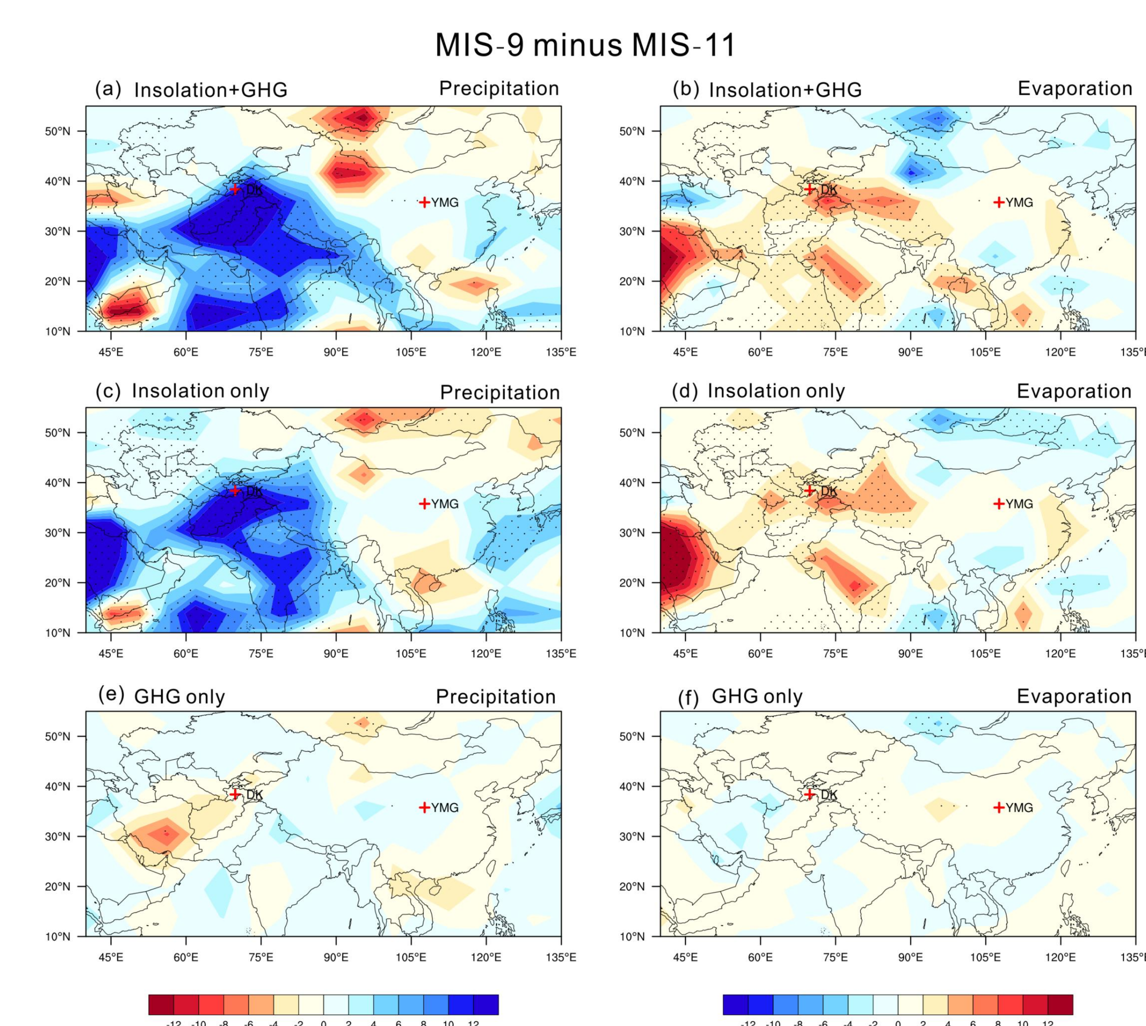

Figure 4. Spatial differences of the annual mean precipitation (cm/yr) and evaporation (cm/yr) between interglacials MIS-9 and MIS-11, respectively, (a) and (b) under the combined effects of insolation and GHG, (c) and (d) of insolation only, and (e) and (f) of GHG only. The blue color represents higher precipitation in (a), (c) and (e), and the red color represents higher evaporation in (b), (d) and (f). Dotted regions indicate that changes are significant at the 0.05 confidence level. The red cross represents DK and YMG sections, respectively.

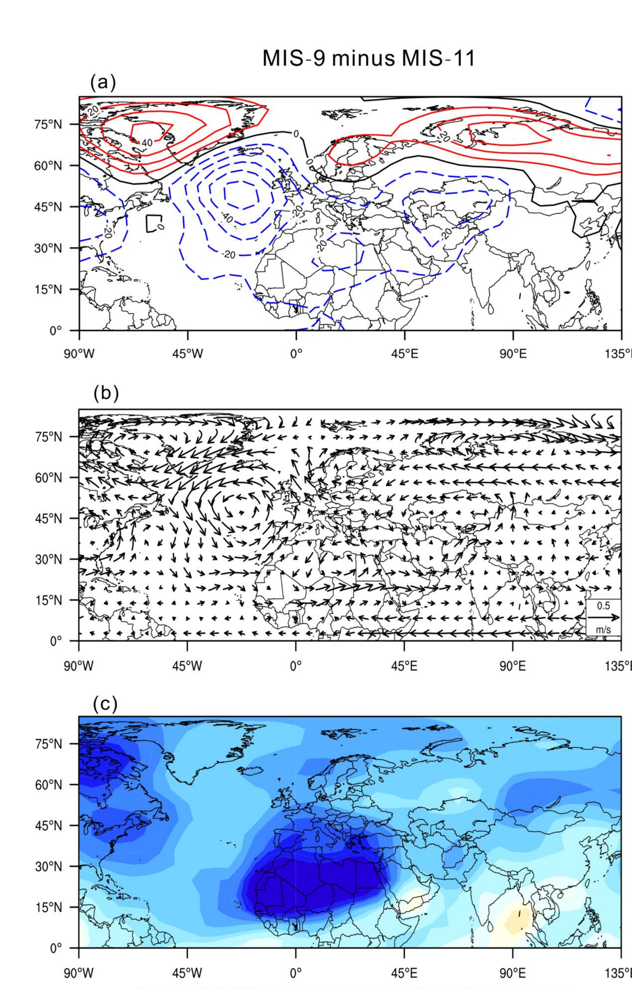

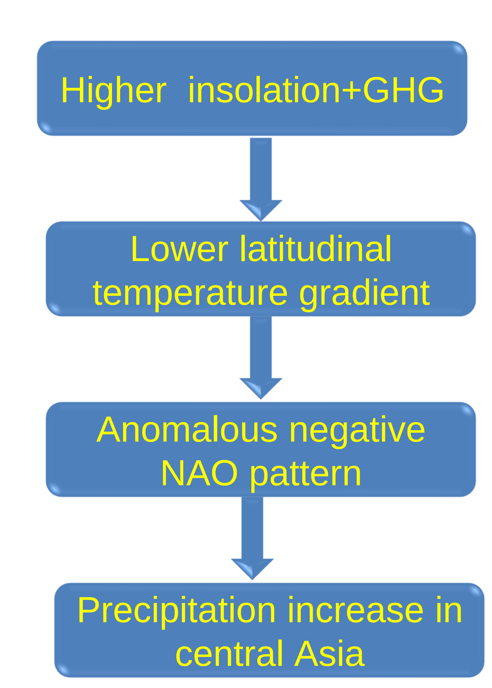

Figure 5. Annual average differences between MIS-9 and MIS-11: (a) geopotenntial height anomalies (m^2/s^2) at 700 hPa; (b) wind field anomalies (m/s) at 700 hPa; (c) surface specific humidity (kg/kg). The red solid line, black solid line and blue dashed line in (a) indicate positive, zero and negative differences, respectively.

4. Conclusions

- **Insolation leads to much more annual mean precipitation than CO_2 during MIS-9 in southern central Asia, explaining a much wetter MIS-9 there as compared to MIS-11.**
- **Both insolation and CO_2 lead to more annual mean precipitation and evaporation during MIS-9 in northern China, leading to a slightly drier MIS-9 than MIS-11.**
- **Higher insolation during MIS-9 lead to precipitation increase in southern central Asia via anomalous atmospheric circulation.**

Literature citation: Lu, H., Yin, Q., Wu, Z., Shi, F., Hao, Q., Xia, D., & Guo, Z. (2022). Insolation and CO_2 impacts on the spatial differences of the MIS-9 and MIS-11 climate between monsoonal China and central Asia. Journal of Geophysical Research: Atmospheres, 127, e2022JD036505. https://doi.org/10.1029/2022JD036505.